Mathematical Problems in Engineering
Volume 3, pp. 287–328
Reprints available directly from the publisher
Photocopying permitted by license only

Identification of Hysteretic Control Influence Operators Representing Smart Actuators Part I: Formulation

H.T. BANKS [a,*,†], A.J. KURDILA [b,c,‡] and G. WEBB [b]

[a] *Center for Research in Scientific Computation, Department of Mathematics, North Carolina State University, Raleigh, NC 27695-8205, USA;* [b] *Department of Aerospace Engineering,* [c] *Department of Mathematics, Texas A&M University, College Station, TX 77843, USA*

(Received 9 May 1996)

A large class of emerging actuation devices and materials exhibit strong hysteresis characteristics during their routine operation. For example, when piezoceramic actuators are operated under the influence of strong electric fields, it is known that the resulting input–output behavior is hysteretic. Likewise, when shape memory alloys are resistively heated to induce phase transformations, the input–output response at the structural level is also known to be strongly hysteretic. This paper investigates the mathematical issues that arise in identifying a class of hysteresis operators that have been employed for modeling both piezoceramic actuation and shape memory alloy actuation. Specifically, the identification of a class of distributed hysteresis operators that arise in the control influence operator of a class of second order evolution equations is investigated. In Part I of this paper we introduce distributed, hysteretic control influence operators derived from smoothed Preisach operators and generalized hysteresis operators derived from results of Krasnoselskii and Pokrovskii. For these classes, the identification problem in which we seek to characterize the hysteretic control influence operator can be expressed as an ouput least square minimization over probability measures defined on a compact subset of a closed half-plane. In Part II of this paper, consistent and convergent approximation methods for identification of the measure characterizing the hysteresis are derived.

Keywords: Hysteretic Preisach operators; Smart materials; Evolution equations; Identification

---

* Corresponding author.

† Research supported in part by the Air Force Office of Scientific Research under grants AFOSR F49620-95-1-0236 and F49620-93-1-0280.

‡ Research supported in part by the Army Research Office under Proposal Number 30378-EG, grant DAAL03-92-012.

1 INTRODUCTION

Research in active, or smart materials, for vibration attenuation, shape control and micro-mechanical actuation is proceeding at a rapid pace. As actuation devices based on the electro-mechanical behavior of piezoceramics and the shape memory alloys have become more widespread, it is now well-appreciated that this class of actuation devices exhibits significant nonlinear response. For example, although the piezoelectric effect is commonly modeled in terms of a linear actuation device [3], it is shown in [11] that hysteresis is routinely observed, and can be accomodated in control design via compensation. The research of [16,14] makes it clear that the response of shape memory alloys at the response scale of the structure is profoundly nonlinear and hysteretic.

To help motivate the discussion of hysteresis modeling that follows in the next section, we consider the results of experiments measuring the structural response of a beam that undergoes deformation under the stress induced in resistively heated shape memory alloy wires. The experimental setup is rather simple. A thin aluminum beam, 1/32 inch in thickness, is cantilevered at one end as depicted in Fig. 1. A "two-way" shape memory alloy wire is attached to the rigid base supporting the cantilevered beam, and to an offset attached to the tip of the free end of the beam. A thermocouple is attached in the center of the length of the shape memory alloy wire, and a strain gauge is attached on the surface of the beam, also at its midpoint. It is clear that with this simple experiment, the temperature (input) to the shape memory alloy wire and the output strain at the surface of the beam can be collected to characterize a temperature-to-strain plant model. Figures 2 and 3 depict the results of a series of experiments wherein the current that resisitively heats the wire is varied. In Fig. 2 (Run A), the current in the wire is held constant at 3 A until a target temperature is achieved, then the current is turned off. As is apparent from the experiment, the major ascent loops and descent loops are strongly hysteretic. In Fig. 2 (Run B), the same protocol in another experimental run is followed, except that the current during activation is 2.5 A. Not only is hysteresis evident, by comparing the response strain-versus-temperature curves to those depicted in Fig. 2, the *family of hysteresis curves* is

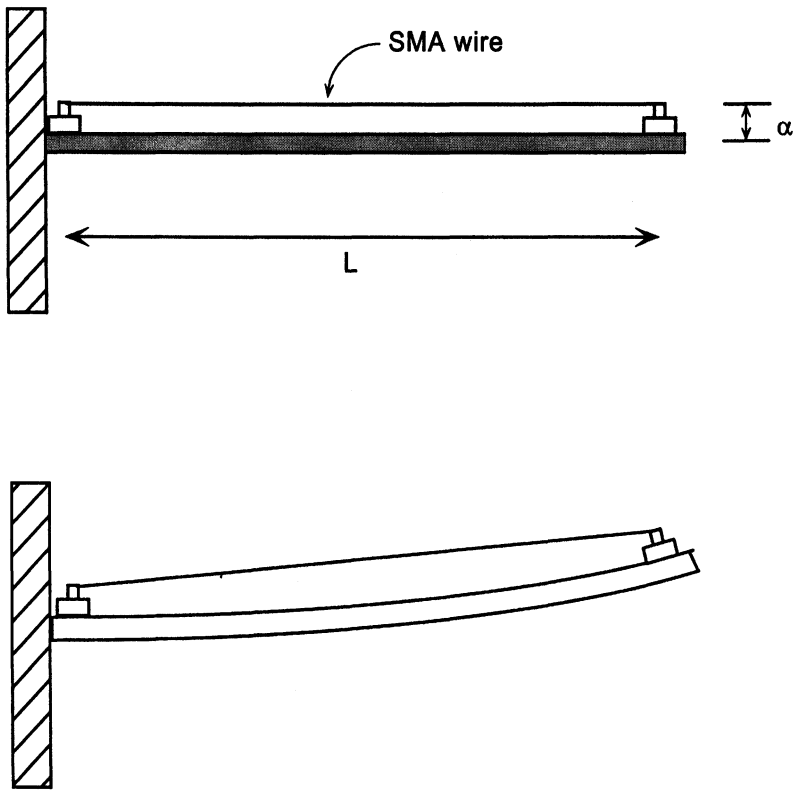

FIGURE 1 Experimental setup.

dependent on the input current. This phenomenon is also evident in Fig. 3, in which the current is varied from 1 to 3 A during the heating cycles.

It has been understood for quite some time that there are two fundamental approaches to mathematically characterizing the input–output behavior of complex dynamical systems. In one approach, researchers model a given system as a collection, or even continuum, of components for which ideal models can be derived from the principles of physics. In the second method, the overall qualitative behaviour of the system as a whole is observed, and some "best representative" is selected from a class of models that exhibit desired, empirically observed, properties. With respect to modeling

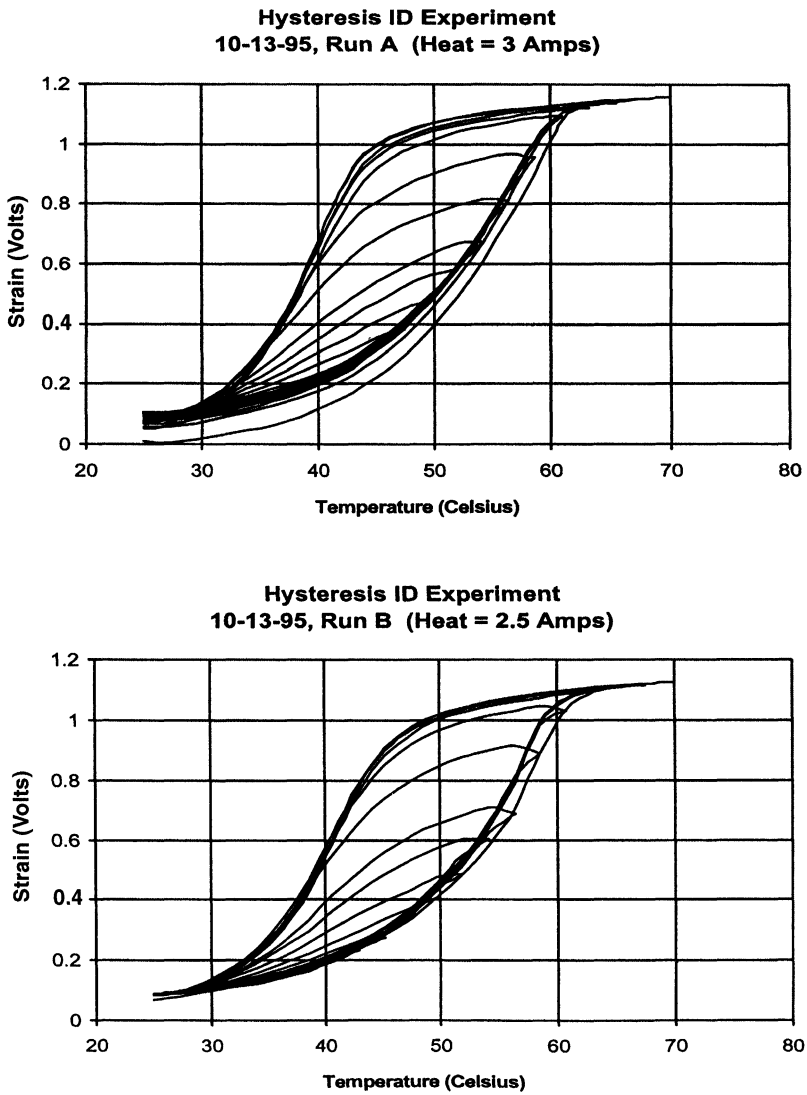

FIGURE 2 Hysteresis in SMA experiments: (a) 3 A, (b) 2.5 A.

hysteresis in active materials, for example, different researchers have formulated constitutive models for shape memory alloys including Liang and Rogers [16], Brinson [9], Barret [6] and Boyd and Lagoudas [8]. The body of research in [16,9,6,8], regarded as a whole, falls

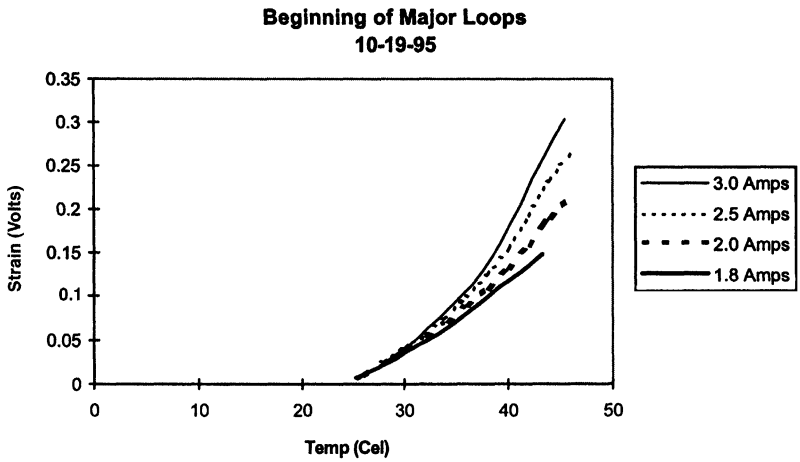

FIGURE 3 Hysteresis in SMA experiments, varying current.

within the first category described above. On the other hand, Hughes and Wen [11] have utilized the Preisach model in a system theoretic sense to represent a static, hysteretic transducer that can be used to derive compensators for controlling shape memory alloy wires. The approach in this paper is also an example of the second, or system theoretic, approach to modeling the response of dynamical systems and is motivated strongly by the work of Hughes and Wen [11]. In this paper we address several mathematical issues that arise in modeling and identification of a class of nonlinear, hysteretic control influence operators in second order evolution operators. We derive two alternative classes of control influence hysteresis operators: (1) the smoothed Preisach operator and (2) the Krasnoselskii–Pokrovskii operator. In Section 2 of this paper, we carefully contrast the physical and mathematical properties of these two classes of control influence operators with those of the classical Preisach operator. We derive some of their continuity properties to lay the foundation for proving the well-posedness of the second order evolution equations presented in Section 3. In Section 4, we introduce a class of error functionals to be used for identification, and we investigate the continuity properties of the mapping from spaces of probability measures characterizing the control influence

operator to the observation error. We rigorously prove that the identification problem is well posed over a larger class of operators than can be represented by the Preisach model of hysteresis alone. In the second part (Banks, Kurdila and Webb, CRSC Technical Report CRSC-TR97-7, N.C. State Univ.) of this two-part paper, we derive consistent and convergent approximation schemes for the identification problem, and compare numerical predictions with experimental results for a class of shape memory alloy actuated structures.

2 CLASSES OF INTEGRAL HYSTERESIS OPERATORS

In this section, we discuss three types of hysteresis operators that are constructed via "parallel connection" or "superposition" of idealized, elementary hysteresis operators. Mathematically, each of the different hysteresis operators is obtained via integration over a class of kernels that embody the elementary hysteresis operators, hence we denote the class of operators as *integral hysteresis operators.* The three types of integral hysteresis operators discussed in this paper are:

1. the classical Preisach operator,
2. the *smoothed* Preisach operator, and
3. the Krasnoselskii–Pokrovskii (KP) operator.

The latter two classes of operators are derived in this paper and are generalizations of the classical Preisach operator. In the discussion that follows, we will denote the kernels of the classical Preisach, the smoothed Preisach and KP operators by $\hat{k}_s$, $\tilde{k}_s$ and κ_s, respectively. The symbol k_s will be used to denote a generic hysteresis kernel, or will refer to the collection of hysteresis kernels without distinguishing its particular form. If we parameterize the kernel k_s, of each hysteresis operator by an element $s \in \mathcal{S}$, where $\mathcal{S}$ is some set of allowable hysteresis parameters in R^2, we can view each of the elementary hysteresis operators as defining a mapping

$$k_s(u, \xi) : C[0, T] \times \mathcal{I} \to \mathcal{F}[0, T],$$

where $u \in C[0, T]$ is the input, $\xi \in \mathcal{I}$ represents the initial condition of the kernel, and $\mathcal{F}[0, T]$ is the function space of outputs. Roughly

speaking, the three elementary hysteresis operators discussed in this paper differ in that they exhibit differing degrees of continuity. Essentially, there are two types of continuity properties of the kernels that are important in this paper. We can consider the continuity of the mapping in *time* given by

$$t \mapsto [k_s(u, \xi)](t)$$

and the continuity of the mapping *in parameter space* given by

$$s \mapsto [k_s(u, \xi)](t).$$

We will see in the following sections that the continuity properties are as summarized in the following table:

Operator type	$t \mapsto [k_s(u,\xi)](t)$ *is continuous*	$s \mapsto [k_s(u,\xi)](t)$ *is continuous*
Classical Preisach $\hat{k}_{s_-}$	No	No
Smoothed Preisach k_s	Yes	No
KP Operator κ_s	Yes	Yes

The property that the operator is continuous in time is important from physical considerations. The parametric continuity of the hysteresis operator is important for developing identification methodologies that are well posed over a large class of *densities or measures* that characterize the hysteresis operator.

2.1 Preisach Model of Hysteresis

Simply put, hysteresis is a nonlinearity characterized by a multivalued mapping, specifically a function with multiple branches. An enormous literature has accumulated over the past few years on models of hysteresis, including the seminal work in [12], and the more recent treatments in [22,18]. Invariably, a discussion of hysteresis draws analogy to the "prototypical" case depicted in Fig. 4. This multivalued function is the delayed relay operator. For input values $u(t)$ that start at a sufficiently small value and increase monotonically, the output response follows the ascent curve shown

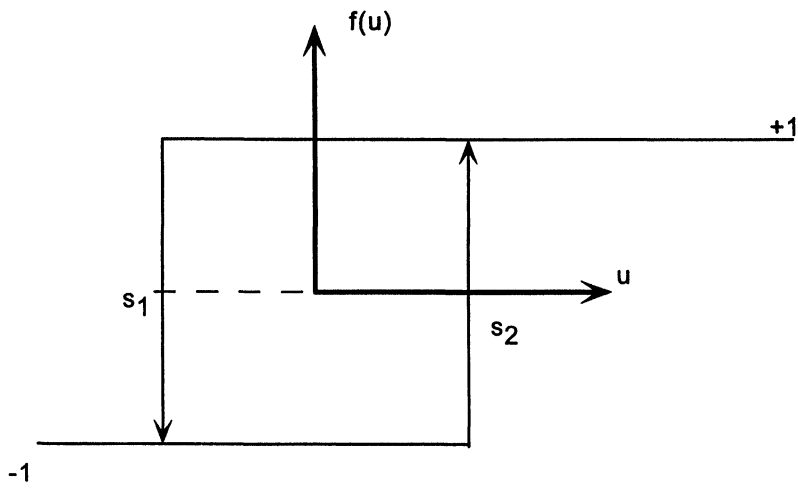

FIGURE 4 Ideal delayed relay operator.

in the figure. That is, the output response begins in a state of "negative saturation" with output -1, and suddenly jumps to a state of positive saturation with output $+1$ when the input $u(t)$ reaches s_2. Likewise, when the input begins at a level that is sufficiently large, the output begins at a value of "positive saturation" equal to $+1$. Upon monotonically decreasing the input $u(t)$, the output jumps to the negative saturation value when the input reaches the switching value of s_1.

While this prototypical case is useful for illustrating that hysteresis is characterized by multiple branches of output and switching points, it is not extremely useful in practice. The model can be generalized, however, so that a reasonable class of practical problems can be treated. The generalization can be interpreted intuitively as the "parallel" connection of a large collection of delayed relay operators. Consider the case when only two delayed relay operators are connected in parallel, as shown in Fig. 5. Clearly, the hysteresis loop in this case is characterized by two jumps in its ascending branch, and two jumps downward in its descending branch. The extension to a finite but large number of parallel-connected delayed relay operators is depicted in Fig. 6.

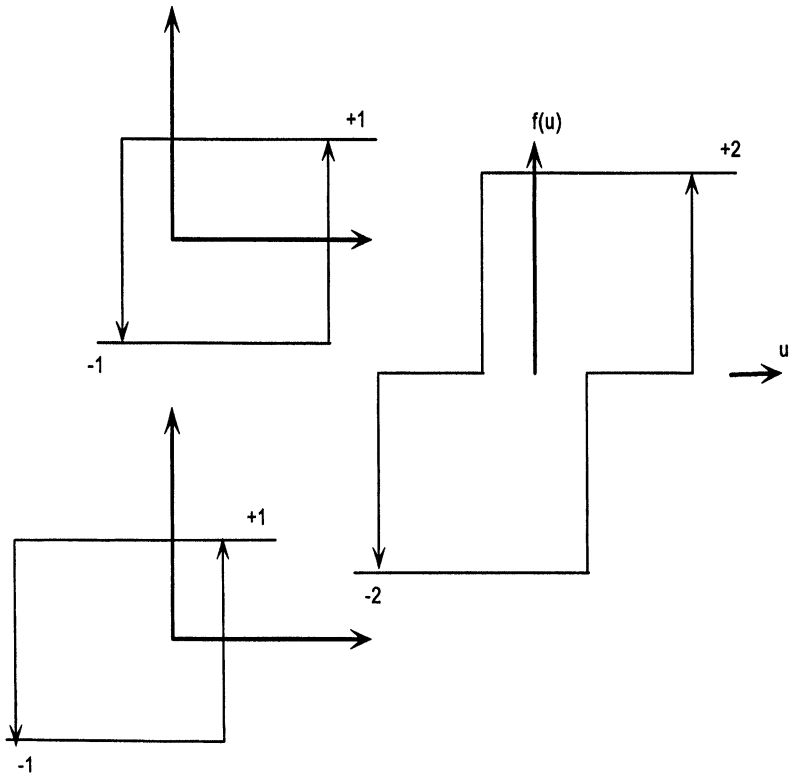

FIGURE 5 Parallel connection, two ideal relays.

In this discussion, we will utilize a generalization that incorporates a distribution of weighted delayed relay operators. To this end, let us define the set of pairs of thresholds that characterize all admissible delayed relay operators

$$\mathcal{S} = \{s \in R^2 \colon s = (s_1, s_2),\ s_1 < s_2\}. \tag{1}$$

Following the development in [22], we define the crossing times $\tau(t)$ associated with the input u and a pair of thresholds $s = (s_1, s_2) \in \mathcal{S}$ by

$$\tau(t) = \{\eta \in (0, t] \colon u(\eta) = s_1 \text{ or } u(\eta) = s_2\}. \tag{2}$$

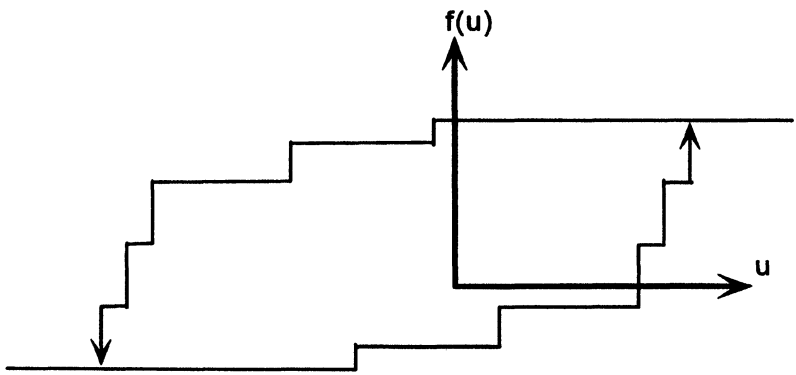

FIGURE 6 Parallel connection, multiple ideal relays.

A single, delayed relay operator is defined by the relationship

$$[\hat{k}_s(u,\xi)](t) \equiv \begin{cases} [\hat{k}_s(u,\xi)](0) & \text{if } \tau(t) = \emptyset, \\ -1 & \text{if } \tau(t) \neq \emptyset \text{ and } u(\max(\tau(t))) = s_1, \\ +1 & \text{if } \tau(t) \neq \emptyset \text{ and } u(\max(\tau(t))) = s_2, \end{cases} \tag{3}$$

where the initial value of the kernel $\hat{k}_s$, is given by

$$[\hat{k}_s(u,\xi)](0) = \begin{cases} -1 & \text{if } u(0) \leq s_1, \\ \xi & \text{if } s_1 < u(0) < s_2, \\ +1 & \text{if } u(0) \geq s_2. \end{cases} \tag{4}$$

We should note that the argument $\xi \in \{-1, 1\}$ defines the initial state of the delayed relay operator, and affects the output of the delayed relay operator only if the input $u(t)$ happens to have an initial value in the open interval (s_1, s_2). Let f be a Borel measurable function mapping $\mathcal{S} \to \{-1, 1\}$ and let $u \in C[0, T]$. We will denote the set of all finite, signed Borel measures on $\mathcal{S} \subset R^2$ by $\mathbb{M}$. For each specific finite, signed Borel measure μ in $\mathbb{M}$, the Preisach operator $\hat{P}_\mu(u, f)$ is defined via

$$[\hat{P}_\mu(u,f)](t) \equiv \int_{\mathcal{S}} [\hat{k}_s(u, f(s))](t)\, \mathrm{d}\mu(s). \tag{5}$$

Under these assumptions, it is shown in [22] that

$$\hat{P}_\mu : C[0,T] \times \mathcal{B}(\mathcal{S}, \{-1,1\}) \rightarrow L_\infty(0,T) \cap C_r[0,T), \tag{6}$$

where $\mathcal{B}(\mathcal{S}, \{-1,1\})$ is the set of all Borel measurable mappings from $\mathcal{S}$ into $\{-1,1\}$, and $C_r[0,T)$ is the set of all right-continuous functions on $[0,T)$.

While the continuity properties of the map

$$t \mapsto [\hat{k}_s(u,\xi)](t)$$

are discussed in detail in [22], it is important in the derivation of the convergent approximation schemes considered in the second part of this paper to establish the continuity of the map

$$s \mapsto [\hat{k}_s(u,\xi)](t).$$

The following lemma provides a motivation for consideration of the more general hysteresis kernels presented in Sections 2.2 and 2.3:

LEMMA 2.1 *Let $\hat{k}_s$ be the delayed relay operator defined in Eqs.* (1)–(4). *Then there exist $u \in C[0,T]$, $\xi\{-1,1\}$ and $t \in [0,T]$ such that the map*

$$s \mapsto [\hat{k}_s(u,\xi)](t)$$

is not continuous.

Proof The proof of this lemma follows by constructing an example. Consider the saw-tooth input function depicted in Fig. 12. This function is simply a piecewise linear spline that oscillates between the values of s_1 and s_2, with period 2. The corresponding output of the delayed relay operator shown in Fig. 13 is piecewise constant. Now consider a sequence of pairs of switching times $\{s_k\}_{k=1}^{\infty}$ where

$$s_k = (s_1, s_2 + 1/k).$$

This family of delayed relay operators is depicted with the dashed lines in Fig. 14. The output of this family of delayed relay operators has the generic form depicted in Fig. 15. Clearly, we have

that

$$s_k \to s = (s_1, s_2) \quad \text{as } k \to \infty,$$

but

$$|[\hat{k}_s(u,\xi)](t) - [\hat{k}_{s_k}(u,\xi)](t)| = 2 \quad \text{for } k = 1, 2, \ldots$$

when $2 \leq t < 3$, $4 \leq t < 5$, etc... This provides the desired counter-example to continuity.

Up to this point, we have only considered time-dependent, real-valued hysteresis operators. In this paper, we treat a class of distributed, hysteretic control influence operators. These Hilbert-space valued operators have the "separable" form

$$\hat{B}_\mu(u,f) \equiv \hat{P}_\mu(u,f) \cdot g, \quad \text{where } g \in V^* \tag{7}$$

and V^* is the topological dual of a Hilbert space V to be defined in the governing system equations. It is not difflcult to argue that this form of governing equation is representative of the actuation force applied by a resistively heated shape memory alloy wire embedded in a rod that undergoes pure bending [13]. To establish the well-posedness of the second order evolution equations presented in Section 3, we must briefly consider some simple regularity properties of B_μ. In the remainder of this paper, we will denote by $\mathbb{A}$ the set of measures $\mathbb{A} \subset \mathbb{M}$ that are absolutely continuous with respect to Lebesgue measure over $\mathcal{S} \subset R^2$.

PROPOSITION 2.1 *If* $u \in C[0,T]$, $f \in \mathcal{B}(\mathcal{S}, \{-1,1\})$ *and* $\mu \in \mathbb{A}$, *then*

$$\hat{B}_\mu(u,f) \in L_2((0,T), V^*). \tag{8}$$

Proof To prove this proposition, we consider the value

$$\|[\hat{B}_\mu(u,f)](t)\|_{V^*} = \sup_{v \in V} \frac{|\int_{\mathcal{S}} [\hat{k}_s(u, f(s))](t)\, \mathrm{d}\mu(s) \cdot g(v)|}{\|v\|_V}$$

at a specific time t. We know this value exists, because if the measure μ is absolutely continuous with respect to Lebesgue measure,

then the Preisach operator is in fact a map

$$\hat{P}_\mu(\cdot, f) : C[0, T] \to C[0, T] \tag{9}$$

as noted in [22]. Thus, in this case the value of the map $\hat{B}_\mu(u, f)$ has the V^* norm

$$\|[\hat{B}_\mu(u, f)](t)\|_{V^*} = |[\hat{P}_\mu(u, f)](t)| \|g\|_{V^*}$$

from which it follows that

$$\|\hat{B}_\mu(u, f)\|^2_{L_2((0,T), V^*)} \leq \max_{t \in [0,T]} \left\{ |[\hat{P}_\mu(u, f)](t)|^2 \right\} \cdot T \cdot \|g\|^2_{V^*}. \tag{10}$$

This completes the proof.

In fact, the control influence operator $\hat{B}_\mu$ is well defined on the larger class $\mathbb{M}$ of finite Borel measures.

PROPOSITION 2.2 *If* $u \in C[0, T]$, $f \in \mathcal{B}(\mathcal{S}, \{-1, 1\})$ *and* $\mu \in \mathbb{M}$, *then*

$$\hat{B}_\mu(u, f) \in L_2((0, T), V^*). \tag{11}$$

Proof This proof follows from the proof of Proposition 2.1, and the fact that if $\mu \in \mathbb{M}$ then $\hat{P}_\mu(u, f) \in L_\infty(0, T) \cap C_r[0, T)$.

2.2 Smoothed Preisach Operators

The Preisach model summarized in the last section has been studied in [12,22,18], and utilized in identification and control in [11]. Various generalizations of the Preisach model have also been studied. For example, [18] presents time-varying Preisach models, as well as vector-valued Preisach models. The discussions in [22,12] introduce convexifications and set-valued versions of the classical Preisach operator. In this section, we derive a different generalization of the Preisach operator that is appealing from physical considerations. In applications to shape memory alloys, the onset and progress of hysteresis is slow. While the Preisach model is attractive in its simplicity, it is questionable whether it is appropriate to model this class of physical hysteresis in terms of jump discontinuities. At this point, it is important to recall (see (9)) that the output of the Preisach operator can be made continuous in time by

restricting attention to the narrow class of measures that can be represented via a probability density as opposed to a probability distribution. On the other hand, for approximation reasons, we would like to consider identification procedures over a larger class of measures, including discrete measures. Thus, in this section we introduce smoothed versions of the Preisach operator. *In addition to being of interest for physical reasons, this class of operators also serves as a conceptual bridge to the more general KP operators discussed in Section* 2.3.

To construct the continuous Preisach operator, we first define a smoothed delayed relay operator as depicted in Fig. 7, each of whose ascending and descending branches are continuous. Let $r(x)$ be a continuous monotone ridge function, as depicted in Fig. 8. As illustrated in Figs. 9 and 10, the constant α characterizes the rise time of the ridge function. We represent the continuous, delayed relay operator in terms of two, shifted images of a single ridge function as depicted in Fig. 11. Unlike the conventional definition, we identify the ascending and descending branches of the model using a selector function h defined by

$$h : \{-1, 1\} \times \mathcal{S} \rightarrow R^1, \tag{12}$$

$$h : (-1, (s_1, s_2)) \mapsto s_2, \tag{13}$$

$$h : (+1, (s_1, s_2)) \mapsto s_1. \tag{14}$$

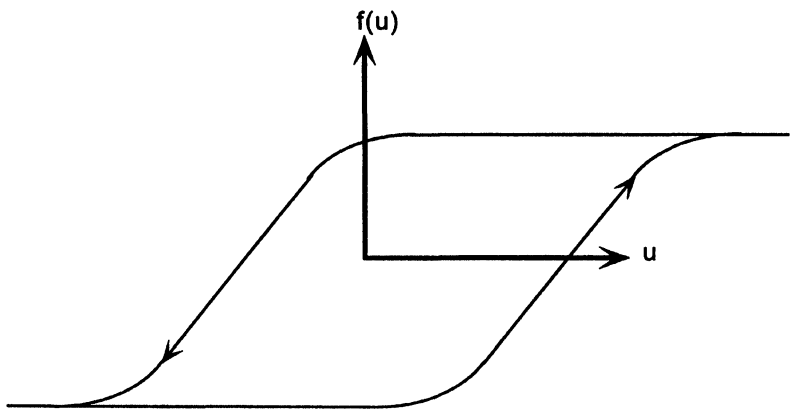

FIGURE 7 Smoothed ideal relay operator.

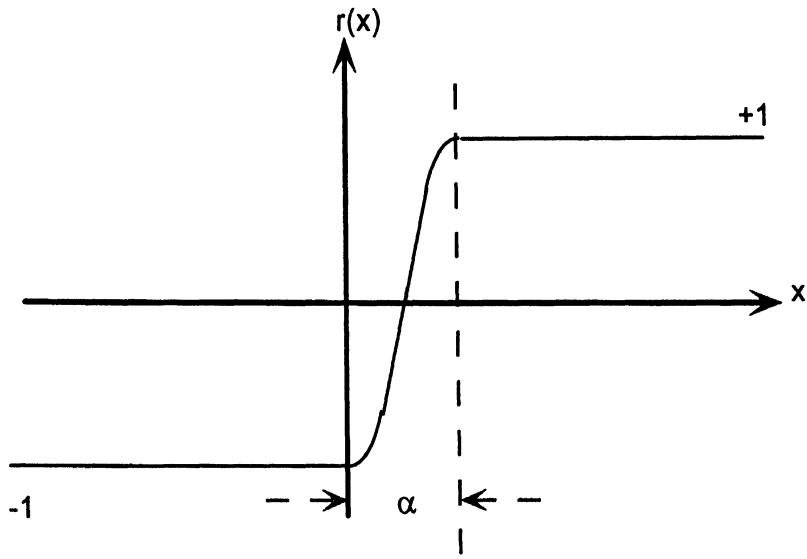

FIGURE 8 Continuous ridge function.

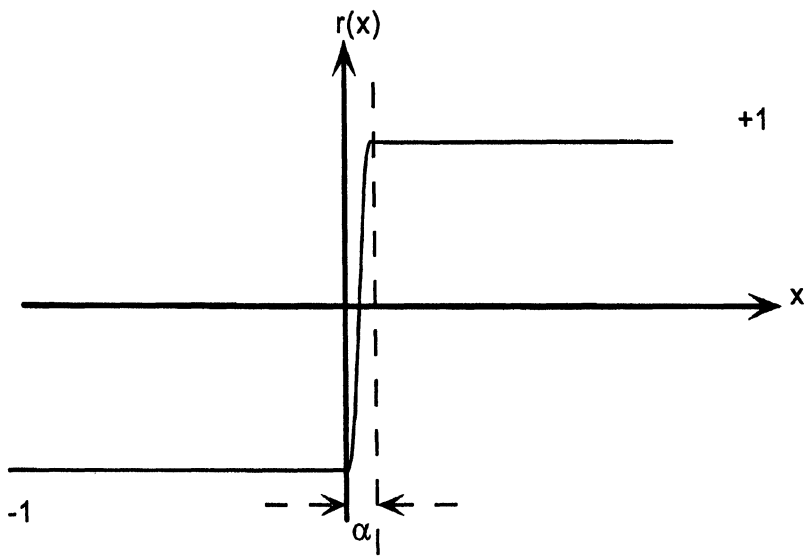

FIGURE 9 Continuous ridge function, short rise time.

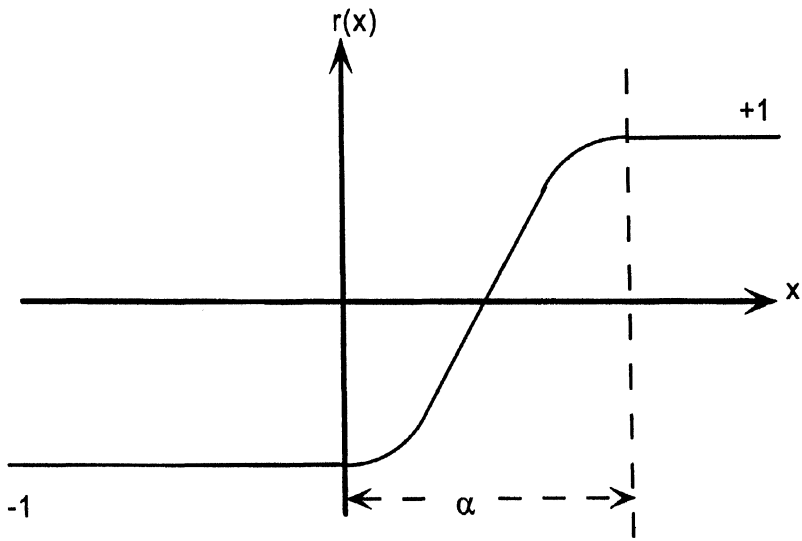

FIGURE 10 Continuous ridge function, long rise time.

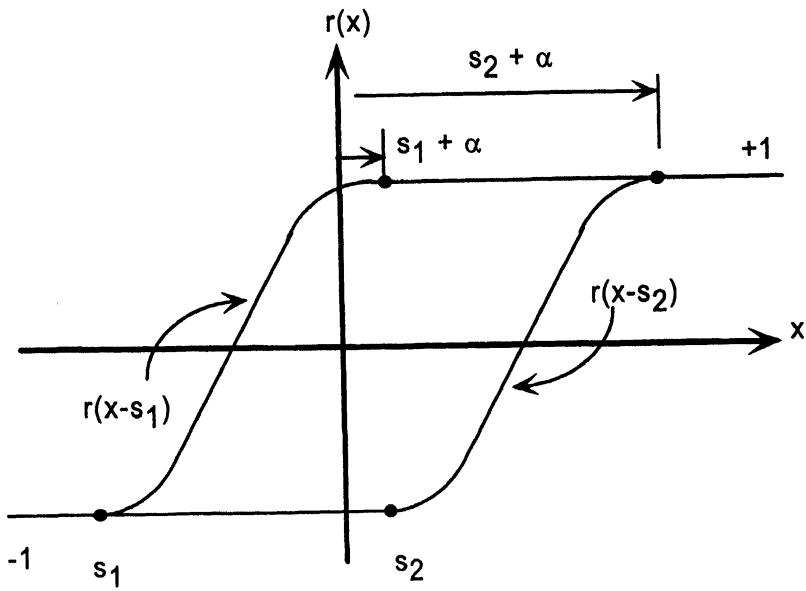

FIGURE 11 Two shifted ridge functions, smoothed relay.

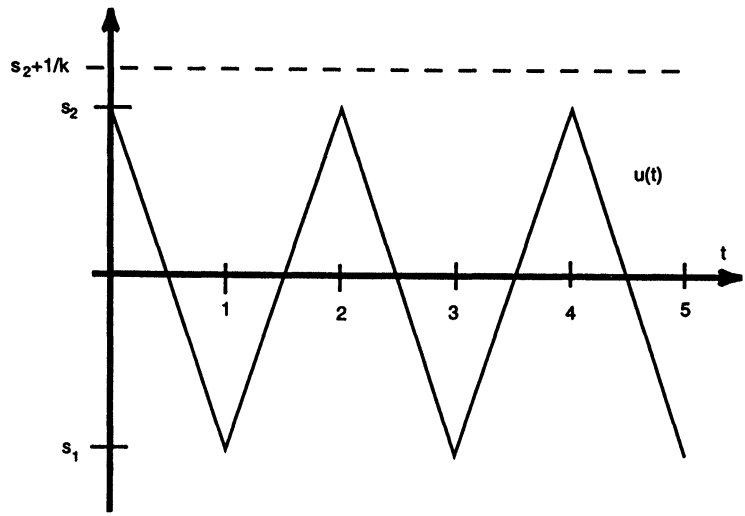

FIGURE 12 Continuous input function $u(t)$.

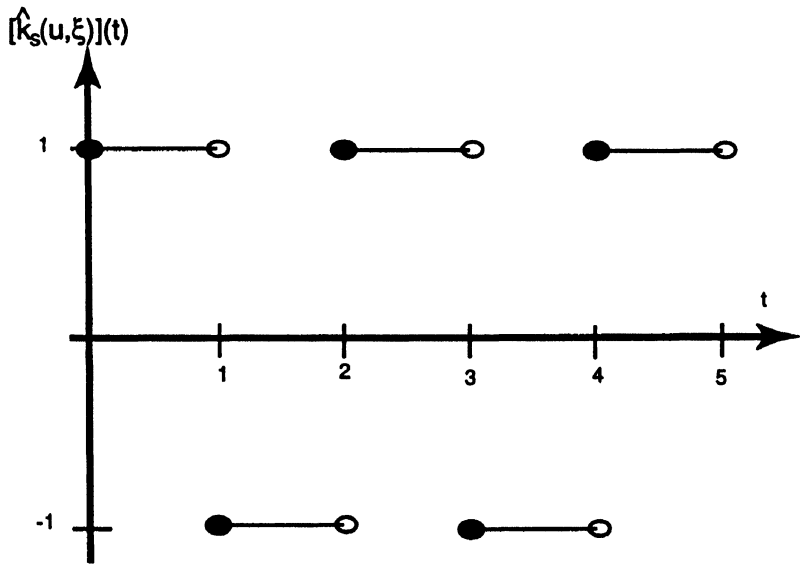

FIGURE 13 Piecewise continuous output function, $s = (s_1, s_2)$.

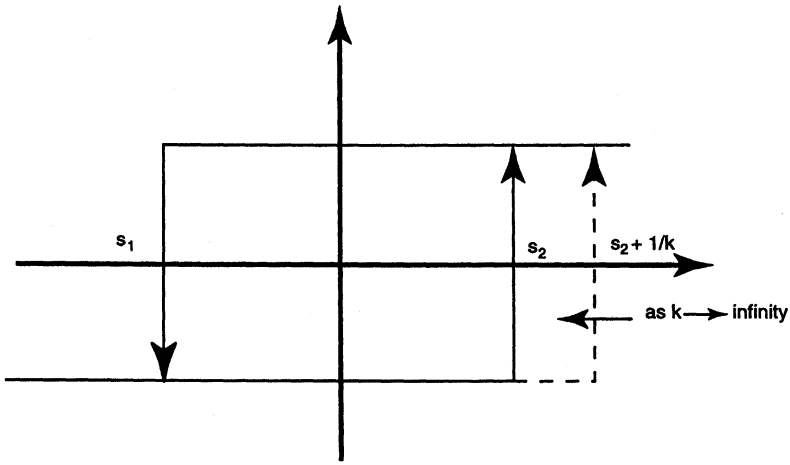

FIGURE 14 Convergent sequence of delayed relay operators.

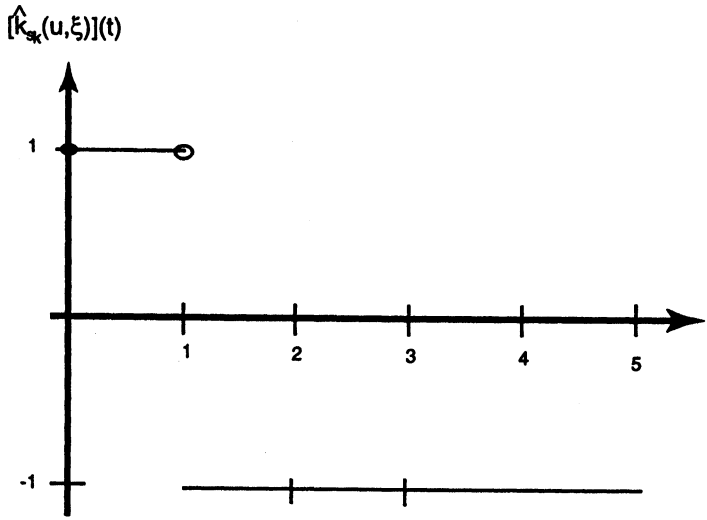

FIGURE 15 Piecewise continuous output function, $s=(s_1, s_2)$.

For any continuous input $u \in C[0, T]$ and any pair $(s_1, s_2) \in \bar{\mathcal{S}}$ with $s_2 \geq s_1$, we can define the crossing times as

$$\tau_s(t) \equiv \{\zeta \in (0, t]: u(\zeta) = s_1 \text{ or } u(\zeta) = s_2 + \alpha\}. \tag{15}$$

Now we can define the initial value of the delayed relay operator

$$[\tilde{k}_s(u, \xi)](0) \equiv r(u(0) - h(\xi, s)). \tag{16}$$

For all $t > 0$, we define

$$[\tilde{k}_s(u, \xi)](t) = \begin{cases} r(u(t) - h(\xi, s)), & \tau_s(t) = \emptyset, \\ r(u(t) - s_1), & \tau_s(t) \neq \emptyset \text{ and } u(\max(\tau_s(t))) = s_2 + \alpha, \\ r(u(t) - s_2), & \tau_s(t) \neq \emptyset \text{ and } u(\max(\tau_s(t))) = s_1. \end{cases} \tag{17}$$

It is important to note that the smoothed Preisach operator, unlike the conventional Preisach operator, can be defined on the closure $\bar{\mathcal{S}}$ of $\mathcal{S}$ in R^2. Careful inspection of Eqs. (2) and (3) shows that it does not make sense to define the classical Preisach operator for $s_1 = s_2$. The smoothed, delayed relay operator defined above has several useful measurability and continuity properties.

THEOREM 2.1 *Let $\tilde{k}_s$ be the delayed relay operator defined in Eqs. (12)–(17). For each $s \in \bar{\mathcal{S}}$ and $\xi \in \{-1, 1\}$, we have*

$$\tilde{k}_s(\cdot, \xi) : C[0, T] \to C[0, T]. \tag{18}$$

Proof The proof of statement (18) is immediate if $s_1 = s_2$ and relatively direct in the case $s_1 > s_2$. If $u \in C[0, T]$, it is a continuous function on a compact set, and consequently, it is uniformly continuous. For any fixed $s = (s_1, s_2) \in \mathcal{S}$, the function u can only oscillate through s_1 and $s_2 + \alpha$ a finite number of times. Hence, $\tilde{k}_s(u, \xi)$ is piecewise comprised of a finite collection of the continuous functions $r(u(t) - s_1)$ and $r(u(t) - s_2)$. By construction, $\tilde{k}_s(u, \xi)$ is continuous at the finite number of times it passes from one branch to another, and is therefore continuous on $[0, T]$.

It is counterintuitive, but despite the "smooth" appearance of the ridge functions comprising the delayed relay $\tilde{k}_s$, the mapping $[\tilde{k}_s(u, \xi)](t)$ is not continuous as we vary $s \in \mathcal{S}$ in *parameter space.*

LEMMA 2.2 *Let $\tilde{k}_s$ be the delayed relay operator defined in Eqs.* (16) *and* (17). *Then there exist $u \in C[0, T]$, $\xi \in \{-1, 1\}$ and $t \in [0, T]$ such that the map*

$$s \mapsto [\tilde{k}_s(u, \xi)](t)$$

is not continuous.

Proof As in the proof of Lemma 2.1, this result follows from a simple counterexample. Consider a saw-tooth input function as depicted in Fig. 16. This function is a piecewise linear spline that oscillates between the values of s_1 and $s_2 + \alpha$. It is a period 2 function. Consider the family of *smoothed* delayed relay operators depicted using the dashed lines in Fig. 17. Each smoothed delayed relay operator is characterized by the shifts

$$s_k = (s_1, s_2 + 1/k).$$

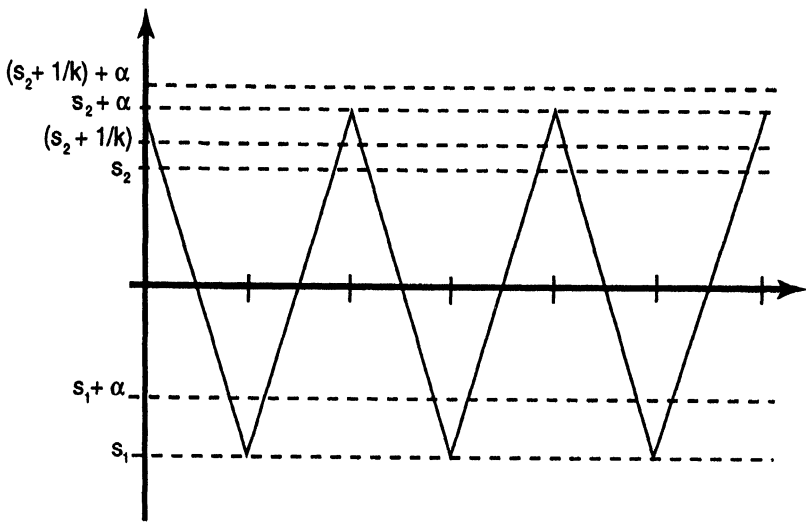

FIGURE 16 Continuous input function.

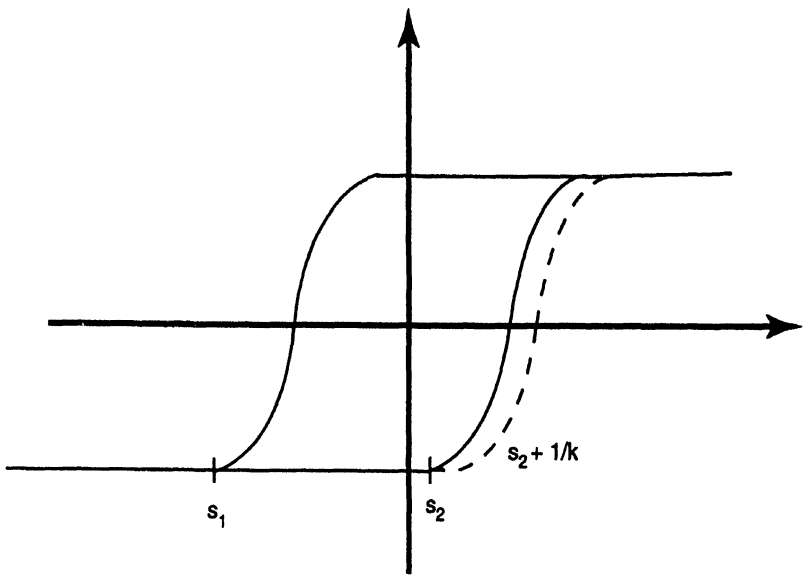

FIGURE 17 Sequence of convergent smoothed relay operators.

Clearly, we have that

$$s_k \to s = (s_1, s_2) \quad \text{as } k \to \infty$$

but there exists a $t = t^* \in (2, 3)$ and an $\epsilon > 0$ such that

$$|[\tilde{k}_s(u, \xi)](t) - [\tilde{k}_{s_k}(u, \xi)](t)| = 2 \quad \text{for } k \geq 1 \text{ and } t \in (t^* - \epsilon, t^* + \epsilon).$$

This can be readily seen from the construction of outputs for $\tilde{k}_s$ and $\tilde{k}_{s_k}$ depicted in Figs. 18 and 19. This completes the proof.

As in the previous section, we formulate the control influence operator by defining the continuous version of the Preisach operator to be

$$[\tilde{P}_\mu(u, f)](t) \equiv \int_{\mathcal{S}} [\tilde{k}_s(u, f(s))](t)\, d\mu(s).$$

The control influence operator is defined using Eq. (7)

$$\tilde{B}_\mu(u, f) \equiv \tilde{P}_\mu(u, f) \cdot g, \tag{19}$$

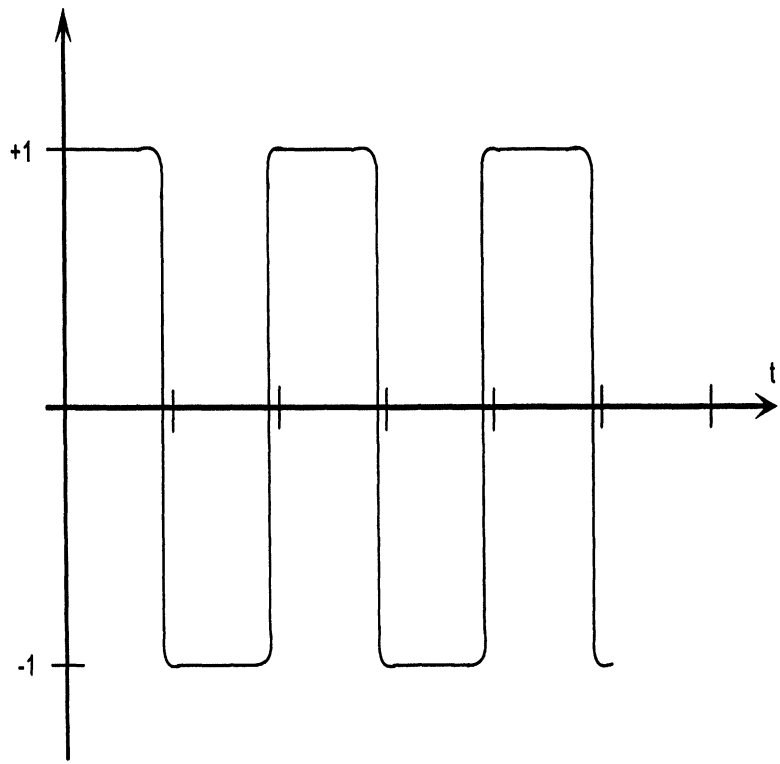

FIGURE 18 Continuous output function, $s=(s_1, s_2)$.

where $g \in V^*$. As in the case of the classical Preisach operator, we will need the following result to guarantee the well-posedness of the governing evolution equations.

PROPOSITION 2.3 *If* $u \in C[0,T]$, $f \in \mathcal{B}(\mathcal{S}, \{-1,1\})$ *and the control influence operator* $\tilde{B}_\mu$ *is defined using Eqs.* (12)–(17), *then*

$$\tilde{B}_\mu(u,f) \in L_2((0,T), V^*) \tag{20}$$

for any $\mu \in \mathbb{M}$.

Proof The proof is identical to the arguments for Propositions 2.1 and 2.2.

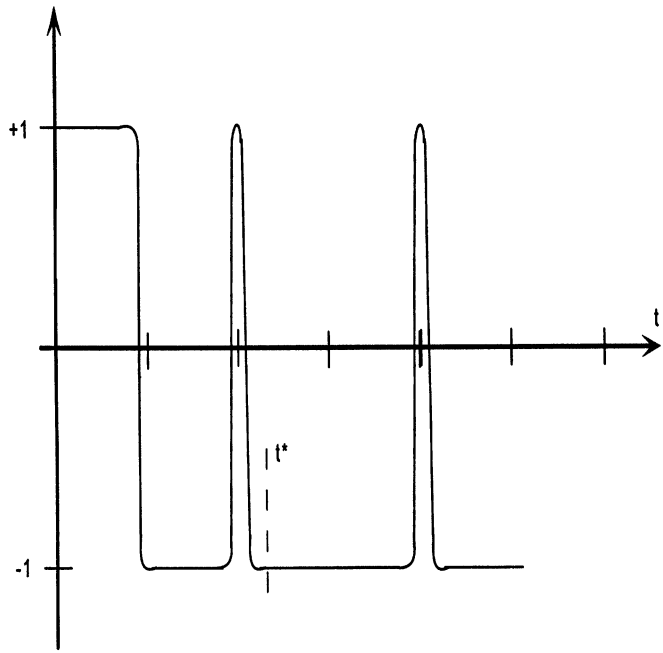

FIGURE 19 Continuous output function, $s_k = (s_1, s_2 + 1/k)$.

2.3 The Krasnoselskii–Pokrovskii Operator

We have seen that the kernel of the smoothed Preisach operator $\tilde{k}_s$ defines a continuous mapping

$$t \mapsto [\tilde{k}_s(u, \xi)](t),$$

whereas the kernel of the Preisach operator is only piecewise continuous in time. Because of the time-continuous nature of the physical phenomenon to be modeled, hysteresis at the structural scale, the smoothed Preisach operator is more suitable for the class of problems of interest. Still, neither the classical nor smoothed Preisach kernels are continuous functions *as we vary the parameters characterizing the prototypical relays*. This property is of critical importance in deriving convergent approximation schemes for the identification problem for the larger class of measures convenient for practical application.

In this section, we introduce another generalization of hysteretic control influence operators by incorporating Krasnoselskii and Pokrovskii's notion of generalized plays. As opposed to considering the KP operators in the full generality discussed in [12], we present a class of KP operators that appear as "natural extensions" of the smoothed Preisach operators discussed in the last section. As depicted in Fig. 11, let $r(x)$ be a *Lipschitz continuous* ridge function and denote its s_1 and s_2 translates by

$$r_{s_1} = r(x - s_1),$$
$$r_{s_2} = r(x - s_2).$$

As opposed to the smoothed relay operator described in Section 2.2, the functions r_{s_1} and r_{s_2} define *the envelope of admissible paths*. The construction of the KP operator for any input $u \in C[0, T]$ proceeds in two steps:

(i) define the KP operator for piecewise monotone (specifically, piecewise continuous) functions, and
(ii) extend the definition by continuity of the dense set of piecewise continuous functions to all of $C[0, T]$.

For the purposes of this paper, the following definition of the KP kernel κ_s will be sufficient. First, for any monotone function $\tilde{u}(t)$, define the monotone output operator by (see Figs. 20, 21)

$$[\mathcal{M}(\tilde{u}, \xi)](t) = \begin{cases} \max\{\xi, r(\tilde{u}(t) - s_2)\} & \text{if } \tilde{u} \text{ is nondecreasing,} \\ \min\{\xi, r(\tilde{u}(t) - s_1)\} & \text{if } \tilde{u} \text{ is nonincreasing.} \end{cases} \tag{21}$$

Now suppose that $\tilde{u}$ is piecewise monotone. Specifically, let $\tilde{u} \in C[0, T] \cap S_{1,j}[0, T]$, where $S_{1,j}[0, T]$ is the set of piecewise linear splines with j knots. We extend the definition of the KP kernel in this case by setting $\mathcal{M}_0 = \xi$ and defining the kernel inductively on each sub-interval (see Figs. 22, 23)

$$[\kappa_s(\tilde{u}, \xi)](t) = \begin{cases} [\mathcal{M}(\tilde{u}, \mathcal{M}_{k-1})](t), & t \in [t_{k-1}, t_k], \\ \mathcal{M}_k = \mathcal{M}(\tilde{u}, \mathcal{M}_{k-1})(t), & k = 1, \ldots, j. \end{cases} \tag{22}$$

For computational purposes, this definition is sufficient. The extension of this definition for all $u \in C[0, T]$ follows from an extension

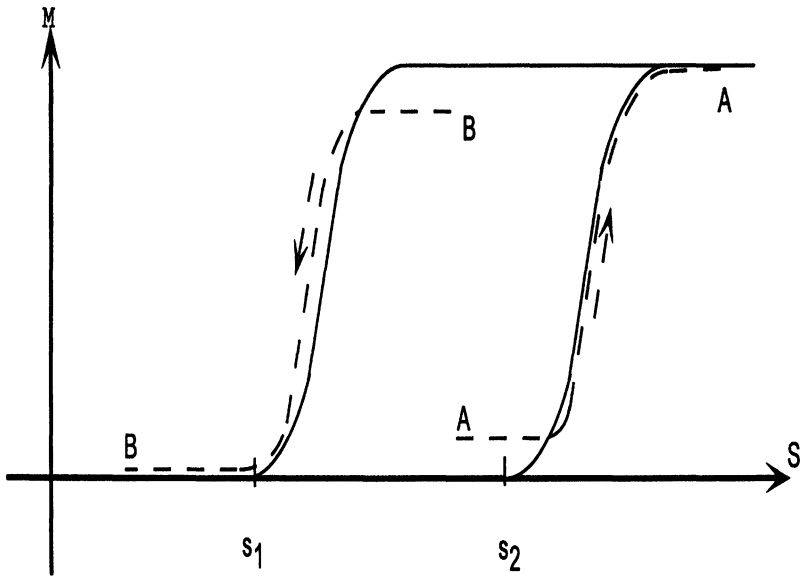

FIGURE 20 KP hysteretic kernel function, output, monotone.

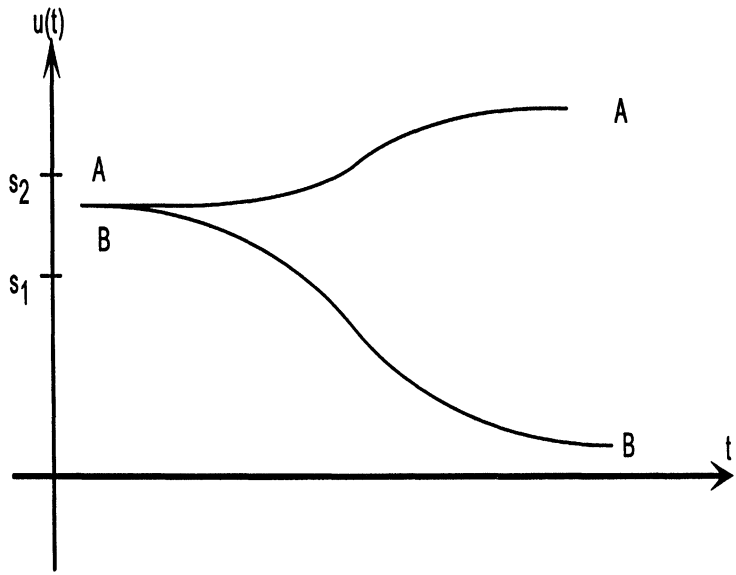

FIGURE 21 KP hysteretic kernel function, input, monotone.

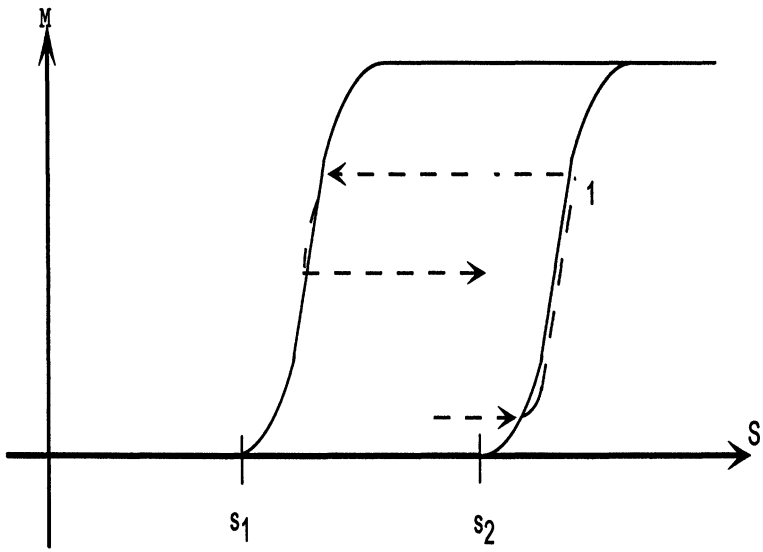

FIGURE 22 KP hysteretic kernel function, output, piecewise monotone.

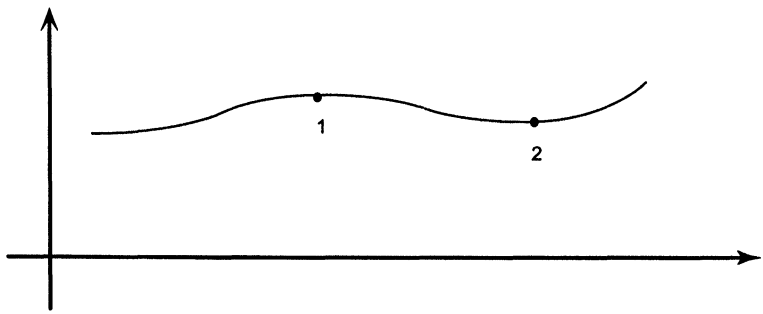

FIGURE 23 KP hysteretic kernel function, input, piecewise monotone.

by continuity argument as discussed in [22] or [12]. The following theorem summarizes the continuity properties of the hysteresis operator generated by the KP kernel:

THEOREM 2.2 *Let κ_s be the KP kernel defined in Eqs.* (21) *and* (22).

1. *For each $s \in \bar{\mathcal{S}}$ and $\xi \in \{-1, 1\}$ we have that*

$$\kappa_s(\cdot, \xi) : C[0, T] \to C[0, T]. \tag{23}$$

2. *For each* $u \in C[0, T]$, $\xi \in \{-1, 1\}$ *and* $t \in [0, T]$ *the map*

$$s \mapsto [\kappa_s(u, \xi)](t) \tag{24}$$

is continuous from $\bar{\mathcal{S}}$ *to* R^1.

3. *If the control influence operator* B_μ *is defined via*

$$B_\mu(u, f) \equiv P_\mu(u, f) \cdot g \equiv \int_{\mathcal{S}} [\kappa_s(u, f(s))](t)\, \mathrm{d}\mu(s) \cdot g, \tag{25}$$

where $g \in V^*$ *and* $\mu \in \mathbb{M}$, *then*

$$B_\mu(u, f) \in L_2((0, T), V^*). \tag{26}$$

Proof The proof of the continuity of the KP kernel operator *as a function of time*, as stated in Eq. (23) above, follows by observing that the generalization of the smoothed Preisach operator introduced in Eqs. (21) and (22) is but a special case of Krasnoselskii and Pokrovskii's definition of generalized play [12]. The curves defining the envelope of output response are, in this case, simply shifts of a single ridge function $r(x)$. The result in Eq. (23) follows from this observation and Theorem 2.2 of [22], page 67.

To prove that the KP kernel operator is continuous in *parameter space*, as noted in Eq. (24), we first note that as $y_k \to y \in R^1$, we have

$$|r(x - y) - r(x - y_k)| \to 0$$

uniformly for $x \in R^1$. This uniform continuity follows directly from the fact that $r(\cdot)$ is Lipschitz continuous on R^1. Thus, given $s_k = (s_{1k}, s_{2k}) \to s = (s_1, s_2)$ in $\bar{\mathcal{S}}$ we have that for any $\epsilon > 0$, we can find $K > 0$ such that

$$|r(x - s_i) - r(x - s_{ik})| \leq \epsilon \quad \text{for } k \geq K,\ x \in R^1 \text{ and } i = 1, 2. \tag{27}$$

The continuity in (24) now follows from Proposition 2.5 of [22], page 70.

The proof of statement (26) follows from (23) and arguments similar to those for Propositions 2.1 and 2.2.

3 SECOND ORDER EVOLUTION EQUATIONS

Based on the experimental setup and initial observations described in the introduction, in this section we will derive governing equations in weak form that incorporate a hysteretic control influence operator. Let V and H be real Hilbert spaces that form a Gelfand triple. That is,

$$V \hookrightarrow H \approx H^* \hookrightarrow V^*.$$

Each of the embeddings $V \hookrightarrow H$ and $H^* \hookrightarrow V^*$ is dense and continuous. The pivot space H is identified with its dual space H^* by the Riesz-mapping. It is well-known that by the construction of the Gelfand triple [23], the duality pairing on $V^* \times V$, denoted by $\langle \cdot, \cdot \rangle_{V^*,V}$, is the extension by continuity of the inner product on H from $V \times H$ to $V^* \times H$. Following [3], we define two parameter dependent operators $A_1(q)$ and $A_0(q)$ that represent the damping and stiffness operators, respectively. The parameters q are assumed to lie in a compact metric space $\mathcal{Q}$. In operator form, the equations governing the dynamics of the system discussed in the introduction have the form

$$\ddot{w}(t) + A_1(q)\dot{w}(t) + A_0(q)w(t) = [B_\mu(u, f)](t) \quad \text{in } V^*, \tag{28}$$

where B_μ denotes one of the operators $\hat{B}_\mu$, $\tilde{B}_\mu$ or B_μ of Section 2. More precisely, we assume that the parameter-dependent, bounded linear operators $A_i(q): V \to V^*$, $i = 0, 1$ are defined in terms of bilinear forms $a_i(q)(\cdot, \cdot)$ defined on $V \times V$, where the action $A_i(q)\phi$ is defined by

$$(A_i(q)\phi)(\psi) = a_i(\phi, \psi), \quad \psi \in V.$$

The operator equation in the dual space V^* can be written in the usual fashion in terms of bilinear forms on $V \times V$ and duality products as

$$\langle \ddot{w}(t), \eta \rangle_{V^*,V} + a_1(q)(\dot{w}(t), \eta) + a_0(q)(w(t), \eta) = \langle [B_\mu(u, f)](t), \eta \rangle_{V^*,V} \tag{29}$$

for all $\eta \in V$.

We obtain a well-posed, second order evolution equation by requiring that the initial conditions satisfy

$$w(0) = w_0 \in V, \tag{30}$$

$$\dot{w}(0) = w_1 \in H \tag{31}$$

and that the *symmetric* bilinear form $a_0(q)(\cdot,\cdot)$ that induces the stiffness operator satisfies the usual conditions of *boundedness*

$$|a_0(q)(u,v)| \leq c_1\|u\|_V\|v\|_V \quad \forall u, v \in V \tag{32}$$

and *V-ellipticity*

$$a_0(q)(u,u) \geq c_2\|u\|_V^2 \tag{33}$$

for constants c_1, c_2 that are independent of the parameters $q \in \mathcal{Q}$. In addition, the bilinear form $a_1(q)(\cdot,\cdot)$ that induces the damping operator satisfies the conditions of *boundedness*

$$|a_1(q)(u,v)| \leq c_3\|u\|_V\|v\|_V \quad \text{for all } u, v \in V \tag{34}$$

and a *Garding inequality*

$$a_1(q)(u,u) + c_4\|u\|_H^2 \geq c_5\|u\|_V^2 \tag{35}$$

for constants $c_3, c_4 \in R^1$ and $c_5 > 0$ that are independent of the parameters $q \in \mathcal{Q}$. The following regularity result is a straightforward consequence of the properties of the hysteretic control influence operators $B_\mu(f,u)$, e.g., see Theorem 2.1 and Remark 2.1 of [3].

THEOREM 3.1 *Suppose that* $u \in C[0,T]$ *and* $f \in \mathcal{B}(\mathcal{S}, \{-1,1\})$. *For each* $(q,\mu) \in \mathcal{Q} \times \mathbb{M}$ *there is a unique solution* $w(q,\mu)$ *to* (29)–(31) *such that*

$$w \in C((0,T),V) \subset L_2((0,T),V),$$
$$\dot{w} \in C((0,T),H) \cap L_2((0,T),V),$$
$$\ddot{w} \in L_2((0,T),V^*).$$

4 ERROR FUNCTIONALS AND CONTINUITY

Equation (29) (or equivalently, Eq. (28)) constitutes the equation governing the input/output behavior of the dynamical system. For purposes of identifying the parameters that characterize the system, we must choose a reasonable measurement, or observation, error functional. Of course, to a large degree, our choice of error functional will be dictated by the actual measurements available to us in the laboratory. Generally speaking, pointwise time and spatial measurements are perhaps the most common class of measurements that are available in an experimental configuration. Distributed or averaged measurements of displacement, stress or strain are becoming available with the increase in popularity of distributed sensors such as piezoceramics [15] and fiber optics [19,20]. Increased use of laser scanning techniques and vision-based image capturing techniques offer additional possibilities. Frequently, one considers an output error functional having the form

$$J(q,\mu) = \frac{1}{2}\sum_{i=1}^{N_1} |w(q,\mu)(t_i) - \tilde{w}_i|_V^2 + \frac{1}{2}\sum_{i=1}^{N_2} |\dot{w}(q,\mu)(t_i) - \tilde{\dot{w}}_i|_H^2. \tag{36}$$

In this case $J(q,\mu)$ is a measure of the error between the displacement $w(q,\mu)$ and velocity $\dot{w}(q,\mu)$ predicted by our model and measurements of surface displacement $\tilde{w}$ and velocity $\tilde{\dot{w}}$ on the structure. A more general error criterion for selecting a model including output least squares functionals can be expressed as

$$J(q,\mu) \equiv \int_0^T j(t, w(q,\mu)(t), \dot{w}(q,\mu)(t))\, \mathrm{d}\nu(t) \tag{37}$$

where ν is a Borel Stieltjes measure.

For the sake of brevity, we will consider this form in the remainder of this paper. The interested reader is referred to [4] for a rather detailed discussion of the treatment of discrete-measurement functionals. While we need not define the precise form of the cost functions, the following two standing assumptions will be crucial in the discussion that follows.

(J1) The kernel function j is piecewise continuous from $t \mapsto j(t, \phi, \psi)$ for all $(\phi, \psi) \in V \times H$;

(J2) The kernel function j is lower-semicontinuous on $V \times H$, uniformly in $t \in [0, T]$.

It is clear that this class of cost functionals includes numerous common choices of output error measures. For example, the common quadratic measure of output error

$$J(q, \mu) = \int_0^T \left\{ \frac{1}{2} |C_1 w(q, \mu)(t) - \tilde{w}|_{Z_1}^2 + \frac{1}{2} |C_2 \dot{w}(q, \mu)(t) - \tilde{\dot{w}}|_{Z_2}^2 \right\} \mathrm{d}t$$

has this form when $C_1 \in \mathcal{L}(V, Z_1)$, $C_2 \in \mathcal{L}(H, Z_2)$ where Z_1, Z_2 are Banach spaces representing measured quantities. Moreover, it is possible to interpret the discrete time cost functional (36) in terms of the general output error expression, if we take the measure ν to be a finite counting measure (i.e., a finite sum of Dirac measures).

Of course, when we study the continuity properties of the map from $\mu \mapsto J(q, \mu)$, it is necessary to choose a topology for the measures μ in the domain of J. To present the continuity properties that follow, let us recall the general form of the control influence operators

$$[B_\mu(u, f)](t) \equiv \int_{\mathcal{S}} [k_s(u, f(s))](t) \, \mathrm{d}\mu(s) \cdot g, \tag{38}$$

where $g \in V^*$. They are defined in terms of a finite Borel measure μ defined on the Preisach plane

$$\mathcal{S} \equiv \{(s_1, s_2) \in R^2 \colon s_1 < s_2\}$$

or its closure $\bar{\mathcal{S}}$. In fact, we will see in Part II of this paper that in practice it is sufficient to limit our considerations to compact subsets $\bar{\mathcal{S}}_\Delta \subset \bar{\mathcal{S}}$ in the integration in Eq. (38). We then have the form

$$[B_\mu(u, f)](t) \equiv \int_{\bar{\mathcal{S}}_\Delta} [k_s(u, f(s))](t) \, \mathrm{d}\mu(s) \cdot g,$$

where $g \in V^*$. Consequently, we will investigate two classes of measures for the study of the continuity properties presented in this section. We will denote by $\mathbb{P}(\mathcal{S})$ the set of all Borel probability

measures on the locally compact, separable metric space $\mathcal{S}$. We endow $\mathbb{P}(\mathcal{S})$ with the topology of weak converge of measures, or convergence in distribution. That is, a sequence $\{\mu_k\}_{k=1}^{\infty} \subset \mathbb{P}(\mathcal{S})$ converges to $\mu \in \mathbb{P}(\mathcal{S})$ if and only if

$$\int_{\mathcal{S}} f \, \mathrm{d}\mu_k \to \int_{\mathcal{S}} f \, \mathrm{d}\mu \tag{39}$$

for all f in the bounded, continuous, real-valued functions $C_b(\mathcal{S})$ on $\mathcal{S}$. From a functional analytic viewpoint, we can regard this as weak* convergence since $\mathbb{P}(\mathcal{S}) \subseteq [C_b(\mathcal{S})]^*$. In an analogous fashion, we define $\mathbb{P}(\bar{\mathcal{S}}_\Delta)$ to be the set of all probability measures over a compact set $\bar{\mathcal{S}}_\Delta = \bar{\mathcal{S}} \cap \{s \in R^2 \colon s = (s_1, s_2), \underline{s} \leq s_1 \leq s_2 \leq \bar{s}\}$ where $\underline{s}$, $\bar{s}$ are finite. It is well-known that $\mathbb{P}(\bar{\mathcal{S}}_\Delta)$ is a compact, metrizable space (see Section 3 of [1] as well as [7,10]).

With this framework in mind, we can establish our first continuity result. In this case, we consider only the properties of the cost as a function of the measure μ; the dependence of the error functional on parameters q appearing in the operators defining the evolution equations has been treated previously in [2].

THEOREM 4.1 *Suppose that the cost functional $J(q, \mu)$ is defined in Eq.* (37), *the solution $w(q, \mu)$ is defined in Eq.* (29), *the control influence operator $\hat{B}_\mu$ is defined in terms of the classical Preisach operator in Eqs.* (5), (7), *and the kernel j of the cost functional satisfies hypothesis* (J1) *and* (J2). *Then for each fixed $q \in \mathcal{Q}$, the map*

$$\mu \mapsto J(q, \mu) \tag{40}$$

is weak lower-semicontinuous from $\mathbb{A} \cup \mathbb{P}(\mathcal{S})$ to R^1.*

Proof By the definition of lower-semicontinuity, we must show that if $\{\mu_k\}_{k=1}^{\infty}$ is a sequence of measures that are absolutely continuous with respect to Lebesgue measure and

$$\mu_k \to \mu_0 \quad \text{weak* in } [C_b(\mathcal{S})]^*, \tag{41}$$

then

$$J(q, \mu_0) \leq \liminf_k J(q, \mu_k).$$

Since all of the measures $\{\mu_k\}_{k=1}^{\infty}$ are absolutely continuous with respect to Lebesgue measure, we know (see [22]) that

$$\hat{P}_{\mu_k}(u,f) \in C[0,T] \quad \forall k = 1,\ldots,\infty.$$

From (8) of Proposition 2.1 we have that

$$\hat{B}_{\mu_k}(u,f) \in L_2((0,T),V^*) \quad \text{for } k = 1,\ldots,\infty.$$

Hence, for each $k=1,\ldots,\infty$, there is a unique solution to the second order evolution equation

$$\langle \ddot{w}_{\mu_k}(t),\eta\rangle + a_1(q)(\dot{w}_{\mu_k}(t),\eta) + a_0(q)(w_{\mu_k}(t),\eta) = \langle [\hat{B}_{\mu_k}(u,f)](t),\eta\rangle$$

subject to the initial conditions

$$w_{\mu_k}(0) = w_0, \quad \dot{w}_{\mu_k}(0) = w_1.$$

Here (and below) we denote $\langle\cdot,\cdot\rangle_{V^*,V}$ by $\langle\cdot,\cdot\rangle$.

There is likewise a unique solution to the evolution equation

$$\langle \ddot{w}_{\mu_0}(t),\eta\rangle + a_1(q)(\dot{w}_{\mu_0}(t),\eta) + a_0(q)(w_{\mu_0}(t),\eta) = \langle [\hat{B}_{\mu_0}(u,f)](t),\eta\rangle$$

subject to the initial conditions

$$w_{\mu_0}(0) = w_0, \quad \dot{w}_{\mu_0}(0) = w_1,$$

where μ_0 is the limit in Eq. (41). If we define the error in approximation to be

$$e_k(t) \equiv w_{\mu_k}(t) - w_{\mu_0}(t), \tag{42}$$

it is clear that the error $e_k(t)$ satisfies the equation

$$\begin{aligned}\langle \ddot{e}_k(t),\eta\rangle + a_1(q)(\dot{e}_k(t),\eta) + a_0(q)(e_k(t),\eta)\\ = \langle [\hat{B}_{\mu_k}(u,f)](t) - [\hat{B}_{\mu_0}(u,f)](t),\eta\rangle\end{aligned} \tag{43}$$

subject to the initial conditions

$$e_k(0) = 0, \quad \dot{e}_k(0) = 0. \tag{44}$$

It is also true that the error $e_k(t)$ satisfies all of the regularity results in Theorem 3.1. In particular, we know that

$$\dot{e}_k \in C((0,T),H) \cap L_2((0,T),V).$$

Thus, we can choose $\eta = \dot{e}_k(t) \in V$ in Eq. (43) to obtain the equation

$$\begin{aligned}&\langle \ddot{e}_k(t), \dot{e}_k(t)\rangle + a_1(q)(\dot{e}_k(t)), \dot{e}_k(t)) + a_0(q)(e_k(t), \dot{e}_k(t))\\ &\quad = \langle [\hat{B}_{\mu_k}(u,f)](t) - [\hat{B}_{\mu_0}(u,f)](t), \dot{e}_k(t)\rangle.\end{aligned}$$

It is important to note that under weaker assumptions (either on the damping operator or on other problem data) on the governing equations, we will not know *a priori* that $\dot{e}_k \in L_2((0,T),V)$. In that case, it would be necessary to follow a slightly modified approach as in [3] or [21]. However, in the case at hand, we can conclude directly that

$$\begin{aligned}&\frac{1}{2}\frac{\mathrm{d}}{\mathrm{d}t}\left(\|\dot{e}_k(t)\|_H^2\right) + a_1(q)(\dot{e}_k(t), \dot{e}_k(t)) + \frac{1}{2}\frac{\mathrm{d}}{\mathrm{d}t}(a_0(q)(e_k(t), e_k(t)))\\ &\quad = \langle [\hat{B}_{\mu_k}(u,f)](t) - [\hat{B}_{\mu_0}(u,f)](t), \dot{e}_k(t)\rangle. \qquad (45)\end{aligned}$$

Integrating once in time, we find that Eq. (45) becomes

$$\begin{aligned}&\|\dot{e}_k(t)\|_H^2 + 2\int_0^t a_1(q)(\dot{e}_k(\tau), \dot{e}_k(\tau))\,\mathrm{d}\tau + a_0(q)(e_k(t), e_k(t))\\ &\quad = \|\dot{e}_k(0)\|_H^2 + a_0(q)(e_k(0), e_k(0))\\ &\qquad + 2\int_0^t \langle [\hat{B}_{\mu_k}(u,f)](\tau) - [\hat{B}_{\mu_0}(u,f)](\tau), \dot{e}_k(\tau)\rangle\,\mathrm{d}\tau. \qquad (46)\end{aligned}$$

To simplify these equations, we use the estimate

$$\begin{aligned}&|\langle [\hat{B}_{\mu_k}(u,f)](\tau) - [\hat{B}_{\mu_0}(u,f)](\tau), \dot{e}_k(\tau)\rangle_{V^*,V}|\\ &\quad \le \|[\hat{B}_{\mu_k}(u,f)](\tau) - [\hat{B}_{\mu_0}(u,f)](\tau)\|_{V^*}\|\dot{e}_k(\tau)\|_V\end{aligned}$$

and employ the standard inequality (for $\alpha > 0$)

$$\|\cdot\|_{V^*}\|\cdot\|_V \le \frac{1}{\sqrt{2\alpha}}\|\cdot\|_{V^*} \cdot \sqrt{2\alpha}\|\cdot\|_V \le \frac{1}{2}\left\{\frac{1}{2\alpha}\|\cdot\|_{V^*}^2 + 2\alpha\|\cdot\|_V^2\right\}.$$

With the use of these inequalities, Eq. (46) can be written

$$\begin{aligned}
&\|\dot{e}_k(t)\|_H^2 + 2\int_0^t a_1(q)(\dot{e}_k(\tau), \dot{e}_k(\tau))\,\mathrm{d}\tau + a_0(e_k(t), e_k(t)) \\
&\quad \le 2\int_0^t \|[\hat{B}_{\mu_k}(u,f)](\tau) - [\hat{B}_{\mu_0}(u,f)](\tau)\|_{V^*}\|\dot{e}_k(\tau)\|_V\,\mathrm{d}\tau \\
&\quad \le \frac{1}{2\alpha}\int_0^t \|[\hat{B}_{\mu_k}(u,f)](\tau) - [\hat{B}_{\mu_0}(u,f)](\tau)\|_{V^*}^2\,\mathrm{d}\tau \\
&\qquad + 2\alpha\int_0^t \|\dot{e}_k(\tau)\|_V^2\,\mathrm{d}\tau.
\end{aligned}$$

Since we assume that the damping bilinear form satisfies a Garding inequality (35) and that a_0 is V-elliptic, we can write

$$\begin{aligned}
&\|\dot{e}_k(t)\|_H^2 + 2c_5\int_0^t \|\dot{e}_k(\tau)\|_V^2\,\mathrm{d}\tau + c_2\|e_k(t)\|_V^2 \\
&\quad \le 2\alpha\int_0^t \|\dot{e}_k(\tau)\|_V^2\,\mathrm{d}\tau + 2c_4\int_0^t \|\dot{e}_k(\tau)\|_H^2\,\mathrm{d}\tau \\
&\qquad + \frac{1}{2\alpha}\int_0^t \|[\hat{B}_{\mu_k}(u,f)](\tau) - [\hat{B}_{\mu_0}(u,f)](\tau)\|_{V^*}^2\,\mathrm{d}\tau. \qquad (47)
\end{aligned}$$

From Theorem 2.5, page 108 of [22], we know that

$$\Delta_k(\tau) \equiv \|[\hat{B}_{\mu_k}(u,f)](\tau) - [\hat{B}_{\mu_0}(u,f)](\tau)\|_{V^*} \to 0 \qquad (48)$$

as $k \to \infty$ for each $\tau \in [0, t]$. Choosing $\alpha = c_5/2$ in (47), we obtain

$$\begin{aligned}
&\|\dot{e}_k(t)\|_H^2 + c_5\int_0^t \|\dot{e}_k(\tau)\|_V^2\,\mathrm{d}\tau + c_2\|e_k(t)\|_V^2 \\
&\quad \le 2c_4\int_0^t \|\dot{e}_k(\tau)\|_H^2\,\mathrm{d}\tau + \frac{1}{c_5}\int_0^t \Delta_k(\tau)\,\mathrm{d}\tau. \qquad (49)
\end{aligned}$$

Ignoring the second and third terms on the left of this inequality, we may use (48) and the usual Gronwall arguments to obtain that $\|\dot{e}_k(t)\|_H \to 0$ as $k \to \infty$, uniformly in $t \in [0, T]$. That is, $\dot{e}_k \to 0$ in $C([0, T], H)$ as $k \to \infty$. Using this along with (49) again, we furthermore obtain $\dot{e}_k \to 0$ in $L_2((0, T), V)$ and $e_k \to 0$ in $C((0, T), V)$ as $k \to \infty$.

From the lower-semicontinuity of j, we have

$$j(t, w_{\mu_0}(t), \dot{w}_{\mu_0}(t)) \leq \liminf_k j(t, w_{\mu_k}(t), \dot{w}_{\mu_k}(t))$$

uniformly in $t \in [0, T]$.

By integrating over time, and using Fatou's Lemma, we obtain

$$J(q, \mu_0) \leq \liminf_k J(q, \mu_k).$$

This completes the proof.

This theorem shows that measures over the Preisach plane $\mathcal{S}$ that are absolutely continuous with respect to Lebesgue measure over $\mathcal{S}$ have at least enough continuity to consider standard techniques, such as in [4,5], to establish the well-posedness of the underlying identification problem. Unfortunately, the subset of measures that are absolutely continuous with respect to Lebesgue measure are not compact in $[C_b(\mathcal{S})]^*$. Thus, to consider an identification procedure that is well-defined, we can modify our class of candidate measures. An obvious choice would be to take *a compact subset* of $[C_b(\mathcal{S})]^*$, including some measures that are not absolutely continuous with respect to Lebesgue measure. But in this case, we may not be able to conclude that

$$|\hat{B}_{\mu_k}(u, f)(\tau) - \hat{B}_{\mu_0}(u, f)(\tau)|_{Y^*} \to 0$$

for each $\tau \in [0, T]$ where $\hat{B}_\mu$ is induced via the classical Preisach operator. Essentially, the difficulty is that it is possible to find a sequence of measures $\{\mu_k\}$ such that

$$\mu_k \to \mu_0 \quad \text{in } [C_b(\mathcal{S})]^*$$

but for which there exists $t \in [0, T]$ such that we *do not* have

$$\hat{P}_{\mu_k}(u, f)(t) \to \hat{P}_{\mu_0}(u, f)(t).$$

For example, consider the input function

$$u(t) = \left(1 - \frac{t}{2\pi}\right) \sin t.$$

Obviously, this function falls within the envelope $1 - t/(2\pi)$ and $\sin t$ and is depicted in Fig. 24. For this example, we also suppose that the initial condition of all of the relays in the Preisach plane are represented by a function $f \in \mathcal{B}(\mathcal{S}, \{-1, 1\})$ that corresponds to the virgin state depicted in Fig. 25. At an instant in time $t_0 \in ((3\pi)/2, 2\pi)$, it is easy to see that the Preisach plane has the "geometry" depicted in Fig. 26. For convenience, choose a bounded subset $\tilde{\mathcal{S}} \subset \bar{\mathcal{S}}$ as shown in Fig. 26, and choose the weak* convergent sequence of Dirac measures $\mu_k = \delta_{s_k}$ where

$$s_k \equiv (-1/4 - 1/k, 1/2).$$

Clearly, we have that $\mu_k \to \delta_{s_0}$ where

$$s_0 \equiv (-1/4, 1/2)$$

and the convergence is weak* convergence of measures.

We note that $f(s_k) = -1$ for $k > 4$ and $f(s_0) = -1$ for all k. Moreover, we have that

$$\int_{\bar{\mathcal{S}}} [\hat{k}_s(u, f)](t_0)\, \mathrm{d}\mu_k(s) = [\hat{k}_{s_k}(u, f(s_k))](t_0) \quad \text{for all } k \geq 1,$$

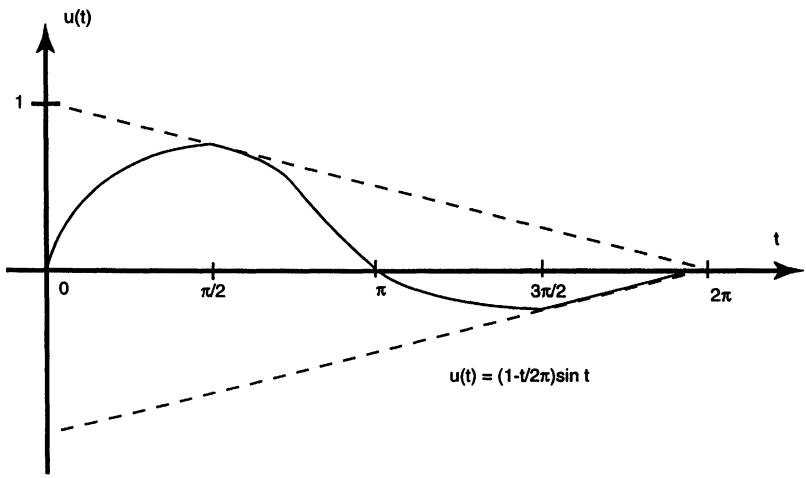

FIGURE 24 Resultant input function.

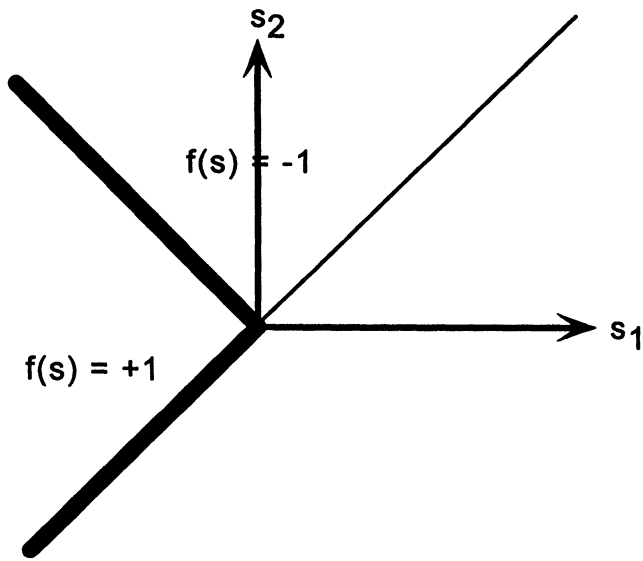

FIGURE 25 Initial, virgin, state in Preisach plane.

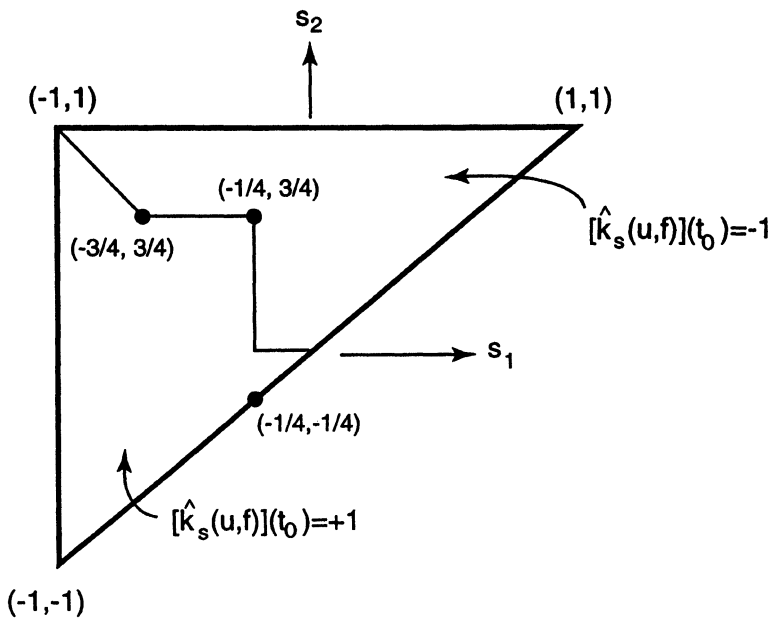

FIGURE 26 Preisach plane geometry at $t = t_0$.

while

$$\int_{\bar{S}} [\hat{k}_s(u,f)](t_0)\,\mathrm{d}\mu_0(s) = [\hat{k}_{s_0}(u,f(s_0))](t_0).$$

But by construction of u, we find $[\hat{k}_{s_k}(u,f(s_k))](t_0) = +1$ for all k and $[\hat{k}_{s_0}(u,f(s_0))](t_0) = -1$. We have consequently constructed an example in which $\mu_k \to \mu_0$ but we do not have

$$\hat{P}_{\mu_k}(u,f)(t_0) \to \hat{P}_{\mu_0}(u,f)(t_0).$$

Indeed, this nonconvergence statement actually holds in a neighborhood $(t_0-\epsilon, t_0+\epsilon)$ of t_0.

However, we can derive a lower-semicontinuity result for the KP integral hysteresis operators introduced in Section 2.3

THEOREM 4.2 *Suppose that the cost functional $J(q,\mu)$ is defined in Eq.* (37), *the solution $w(q,\mu)$ is defined in Eq.* (29), *the control influence operator B_μ is defined in terms of the KP kernel operator in Eqs.* (21), (22), *and the kernel j of the cost functional satisfies hypotheses* (J1) *and* (J2). *Then for each fixed $q \in \mathcal{Q}$, the map*

$$\mu \mapsto J(q,\mu) \tag{50}$$

is weak lower-semicontinuous from $[C_b(\mathcal{S})]^*$ to R^1.*

Proof The proof of this theorem is similar to that of Theorem 4.1, and we only outline the result. We must show that if $\mu_k \to \mu_0$ in $[C_b(\mathcal{S})]^*$ then $J(q,\mu_0) \le \liminf_k J(q,\mu_k)$. But by Proposition 4.1, $B_{\mu_k}(u,f) \in L_2((0,T),V^*)$ for each k. Following the proof of Theorem 4.1, we can deduce that (recall (49))

$$\begin{aligned}
&\|\dot{e}_k(t)\|_H^2 + c_5 \int_0^t \|\dot{e}_k(\tau)\|_V^2\,\mathrm{d}\tau + c_2\|e_k(t)\|_V^2 \\
&\quad \le 2c_4 \int_0^t \|\dot{e}_k(\tau)\|_H^2\,\mathrm{d}\tau \\
&\qquad + \frac{1}{c_5}\int_0^t \|[B_{\mu_k}(u,f)](\tau) - [B_{\mu_0}(u,f)](\tau)\|_{V^*}^2\,\mathrm{d}\tau.
\end{aligned}$$

In the proof of Theorem 4.1, we employed the absolute continuity of the measures μ_k and μ_0 to obtain the desired convergence. Here, however, we have

$$|[B_{\mu_k}(u,f)](\tau) - [B_{\mu_0}(u,f)](\tau)|_{Y^*} \to 0$$

as $k \to \infty$ by the definition of weak* convergence in $[C_b(\mathcal{S})]^*$ and the fact that the KP kernel operator is a continuous map from $\bar{\mathcal{S}}$ to R^1 as noted in Eq. (24) of Theorem 2.2. The remainder of the proof is identical to that in Theorem 4.1.

The advantage of using the KP integral hysteresis operators is now obvious; they induce the required semicontinuity results in the control influence operators B_μ. In addition, these continuity results hold on compact subsets $\mathbb{P}(\bar{\mathcal{S}}_\Delta)$ of $[C_b(\bar{\mathcal{S}}_\Delta)]^*$. The following theorem is the primary contribution of this paper; it states that the identification problem associated with characterizing the hysteretic control influence operator is well-posed for the KP class of kernels *and a wide class of measures.*

THEOREM 4.3 *Suppose that the kernel j of the functional $J(q,\mu)$ satisfies the hypotheses* (J1) *and* (J2), *B_μ is the control influence operator induced by the KP kernel operator defined in Eqs.* (21) *and* (22), *and $w(q,\mu)$ is the solution of the second order governing evolution equations given in Eq.* (29). *If $\bar{\mathcal{S}}_\Delta$ is a compact subset of $\bar{\mathcal{S}}$, then there is a probability measure $\mu_0 \in \mathbb{P}(\bar{\mathcal{S}}_\Delta)$ that solves the hysteretic control influence operator identification problem*

$$J(q,\mu_0) = \inf_{\mu \in \mathbb{P}(\bar{\mathcal{S}}_\Delta)} J(q,\mu).$$

Proof We have already shown in Theorem (4.2) that the map

$$\mu \mapsto J(q,\mu)$$

is weak* lower-semicontinuous from $[C_b(\mathcal{S})]^*$ to R^1. But $\mathbb{P}(\mathcal{S}_\Delta)$ is a compact subset of $[C_b(\bar{\mathcal{S}}_\Delta)]^*$. The desired result then follows since a lower-semicontinuous function on a compact set attains its minimum [17].

This result plays a fundamental role in convergence and approximation results related to the identification of hysteretic control influence operators. First, it guarantees existence of a solution to the identification problem over a very general class of measures. More importantly for computational purposes, from Theorem 3.3 of [1] we have that the set of finite linear combinations of Dirac delta measures $\mu_s = \delta_s$ corresponding to $\{s \in \bar{\mathcal{S}}_\Delta : s \text{ rational}\}$ is dense in $\mathbb{P}(\bar{\mathcal{S}}_\Delta)$. Thus any desired measure $\mu_0 \in \mathbb{P}(\bar{\mathcal{S}}_\Delta)$ can be readily approximated by measures that are extremely simple to use in computations.

5 CONCLUSIONS AND FUTURE RESEARCH

To provide a rich foundation for modeling and identification of hysteresis in actuation devices, this paper has introduced two generalizations of the classical Preisach model of hysteresis. The continuous Preisach model yields a continuous output hysteresis, even for measures that are not absolutely continuous with respect to Lebesgue measure. Moreover, the KP hysteretic control influence operator yields both a time-continuous and a parametrically continuous integral hysteresis operator. Continuity and semicontinuity results are established for the integral hysteresis operators derived in this paper. It is shown that the output least squares identification problem for the measure μ characterizing the hysteresis operator is well-posed for a large collection of measures, including discrete measures. The continuity, compactness and well-posedness results derived in this paper form the foundation of convergent approximation schemes discussed in Part II of this paper. Numerical approximation methods and experimental results for a class of shape memory alloys will also be presented in those discussions.

References

[1] H.T. Banks and B.G. Fitzpatrick, Estimation of growth rate distributions in size structured population models, *Quart. Appl. Math.*, **49** (1991) 215–235.

[2] H.T. Banks and K. Ito, A unified framework for approximation in inverse problems for distributed parameter systems, *Control Theory and Advanced Technology*, **4** (1988) 73–90.

[3] H.T. Banks, K. Ito and Y. Wang, Well-posedness for damped second order systems with unbounded input operators, *Technical Report*, CRSC-TR93-10, 1993; *Differential and Integral Equations*, **8** (1995) 587–606.
[4] H.T. Banks and K. Kunisch, *Estimation Techniques for Distributed Parameter Systems*, Birkhäuser, Boston, 1989.
[5] Viorel Barbu, *Analysis and Control of Nonlinear Infinite Dimensional Systems*, Academic Press, Inc., 1995.
[6] D. Barret, Thermomechanical constitutive laws for shape memory alloys, preprint, 1994.
[7] P. Billingsley, *Convergence of Probability Measures*, Wiley, New York, 1968.
[8] J. Boyd and D. Lagoudas, Thermodynamical models for constitutive laws of shape memory alloys, preprint, 1995.
[9] C. Brinson Constitutive laws for control of shape memory alloys, preprint, 1995.
[10] S.N. Ethier and T.G. Kurtz, *Markov Processes: Characterization and Convergence*, Wiley, New York, 1986.
[11] D. Hughes and J.T. Wen, Preisach modeling of piezoceramic hysteresis; independent stress effect, *SPIE*, **2442** (1994) 328–336.
[12] M. Krasnoselskii and A. Pokrovskii, *Systems with Hysteresis*, Nauka, Moscow, 1983; Springer-Verlag, Inc., 1989.
[13] A.J. Kurdila and G. Webb, Identification of thermal and hysteretic response of sma embedded flexible rods, *Proceedings of the Society for Engineering Science*, 1994.
[14] D.C. Lagoudas, Z. Bo, A.J. Kurdila and G. Webb, Identification for a class of nonlinear models for sma embedded elastomer rods, in *Active Materials and Smart Structures*, G.L. Anderson and D.C. Lagoudas (Eds.) **2427** (1995) 93–106.
[15] C.K. Lee, Piezoceramic plates and shells, *Proceedings of the ASME* (1993) 1–10.
[16] C. Liang and C.A. Rogers, One-dimensional thermomechanical constitutive relations of shape memory materials, *Journal of Intelligent Material Systems and Structures*, **1** (1990) 1–20.
[17] D.B. Luenberger, *Optimization by Vector Space*, John Wiley and Sons, 1969.
[18] I.D. Mayergoyz, *Mathematical Models of Hysteresis*, Springer-Verlag, Inc., 1991.
[19] A. Sirkis, Advances in fiber optic sensors, *ARO Workshop on Smart Materials*, University of Maryland, 1995.
[20] H. Taylor, Advances in Fabry–Perot optical sensors, private communication.
[21] R. Temam, *Infinite Dimensional Dynamical Systems in Mechanics and Physics*, Springer-Verlag, Inc., 1988.
[22] Augusto Visintin, *Differential Models of Hysteresis*, Springer-Verlag, Inc., 1994.
[23] J. Wloka, *Partial Differential Equations*, Cambridge University Press, 1987.